Journal of ASTM International, Vol. 7, No. 5
Paper ID JAI103008
Available online at www.astm.org

C. Coleman,[1] *V. Grigoriev,*[2] *V. Inozemtsev,*[3] *V. Markelov,*[4] *M. Roth,*[5] *V. Makarevicius,*[6] *Y. S. Kim,*[7] *Kanwar Liaqat Ali,*[8] *J. K. Chakravarrty,*[9] *R. Mizrahi,*[10] *and R. Lalgudi*[11]

The Effect of Microstructure on Delayed Hydride Cracking Behavior of Zircaloy-4 Fuel Cladding—An International Atomic Energy Agency Coordinated Research Program

ABSTRACT: The rate of delayed hydride cracking (DHC) has been measured in Zircaloy-4 fuel cladding in several metallurgical conditions using the pin-loading tension technique. In light water reactor (LWR) cladding in the cold-worked and cold-worked and stress-relieved conditions, the cracking rate followed Arrhenius behavior up to about 280 °C, but at higher temperatures the rate declined with no cracking above 300°C. Non-LWR cladding appeared to behave in the same manner. In LWR cladding in the recrystallized condition, the cracking rate was highly variable because it depended on K_I within the test range up to 25 $MPa\sqrt{m}$, whereas in the other LWR claddings, cracking rate was independent of K_I, indicating that K_{IH} was below 11 $MPa\sqrt{m}$. The main role of microstructure was to control the material strength; the cracking rate increased as the strength increased. Although all the claddings had a radial texture, it did not protect the cladding from DHC. The DHC fracture surface consisted of flat broken hydrides, often in arcs, but no striations were observed, except in one specimen subjected to thermal cycles.

KEYWORDS: Zircaloy-4 fuel cladding, delayed hydride cracking (DHC), pin-loading tension (PLT), microstructure, temperature dependence, K_I dependence

Introduction

Like other hydride-forming metals, zirconium is susceptible to embrittlement by hydrogen when hydrides are formed [1]. The embrittlement takes two forms: Short-term loss of toughness and a stable time-dependent crack growth mechanism called delayed hydride cracking (DHC). During DHC, hydrides nucleate and grow slowly in the high stress region of a stress-raiser such as a crack tip. When they reach a critical condition, probably related to size, they fracture, the crack extends, and the process is repeated. The characteristics of the mechanism are the following.

- Time is often required between the imposition of stress and the start of cracking. This period is called the incubation time.
- Loading must exceed a threshold condition for cracking, often characterized as K_{IH}. The rate of any subsequent cracking, V, is almost independent of K_I.

Manuscript received January 30, 2010; accepted for publication April 8, 2010; published online June 2010.
[1] Researcher Emeritus, Chalk River Laboratories (CRL), AECL, Chalk River, ON K0J 1J0, Canada, e-mail: colemanc@aecl.ca
[2] Senior Specialist, Studsvik Nuclear AB, SE-611 82 Nyköping, Sweden.
[3] Nuclear Fuel Specialist, International Atomic Energy Agency (IAEA), Wagramer Strasse 5, P.O. Box 100, Vienna 1400, Austria.
[4] Head of Department, The Joint Stock Company A. A. Bochvar High-Technology Research Institute of Inorganic Materials (JSC VNIINM), 5a Rogov St., Moscow 123098, Russia.
[5] Head, Materials Testing Group, Institute for Nuclear Research (INR), Romanian Authority for Nuclear Activities (RAAN), Campului St., No. 1, 115400 Mioveni, P.O. Box 78, Piteşti, Romania.
[6] Senior Researcher, Laboratory of Materials Research and Testing, Lithuanian Energy Institute (LEI), Breslaujos str. 3, LT-44403 Kaunas, Lithuania.
[7] Head, Zirconium Team, Korea Atomic Energy Research Institute (KAERI), Daejeon 305-353, Korea.
[8] Senior Researcher, Pakistan Institute of Nuclear Science and Technology (PINST), P.O. Nilore, Islamabad, Pakistan.
[9] Head, Mechanical Metallurgy Section, Materials Group, Bhabha Atomic Research Centre (BARC), Mumbai 400-085, India.
[10] Senior Researcher, Materials Dept., National Atomic Energy Commission (CNEA-CAC), Av. Gral. Paz 1499, B1650KNA San Martín, Pcia. de Buenos Aires, Argentina.
[11] General Manager, Materials Science and Technology Centre, Energy and Nuclear Research Institute (ENRI), Av. Prof. Lineu Prestes 2242, Cidade Universitària 05508-000, C.P. 11049, Sao Paulo, Brazil.

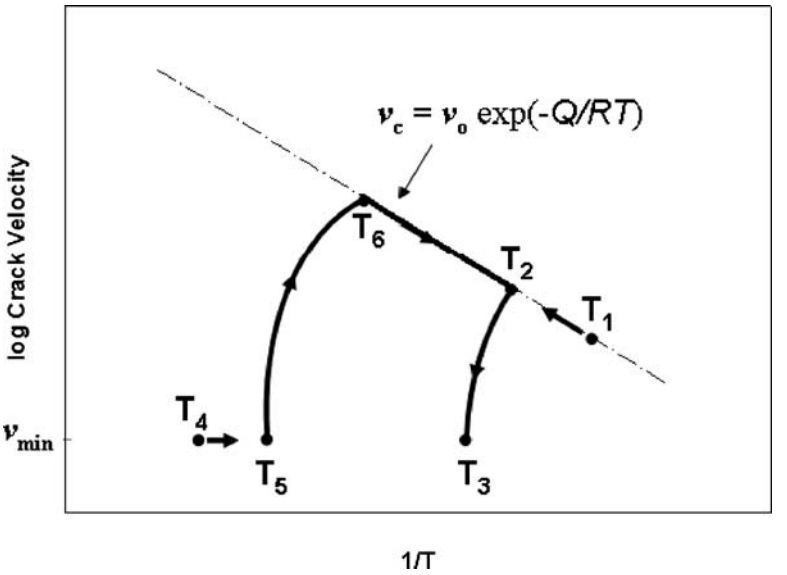

FIG. 1—*Temperature dependence of DHC in zirconium alloys, showing the importance of temperature history on cracking rate.*

- The temperature dependence of cracking is complicated and is described in the schematic diagram depicted in Fig. 1 [2]. The maximum value of V has an apparent Arrhenius behavior and follows

$$V = A \exp(-Q/RT) \tag{1}$$

where:

Q = activation energy for DHC in kJ/mol,
R = gas constant (8.314 kJ/mol K),
T = temperature in K, and
A = constant.

If the temperature is attained by heating from T_1, initially V follows Eq 1, but as the temperature is increased, V starts to decline at T_2 and cracking eventually stops at T_3. On cooling from a high temperature, T_4, a temperature is reached where cracking will reinitiate, T_5, and reach a maximum value at T_6; at lower temperatures V follows Eq 1.

- The amount of hydrogen present in the material should be sufficient for hydrides to be precipitated at the crack tip.
- The material microstructure may affect V through its effect on the diffusivity of hydrogen, material strength, and mode of hydride precipitation, for example, through crystallographic texture.
- A sharp decline in DHC is observed at high test temperatures despite the temperature being attained by cooling and sufficient hydrogen being present to form hydrides. In Zr–2.5Nb the upper temperature limit, T_0, is about 310°C [3].

In components, time-dependent cracking was discovered during the storage at room temperature of Zr–2.5Nb fuel cladding before irradiation [4]. High residual stresses from welding were an important factor in these fractures. High residual stresses were also responsible for cracking in Zr–2.5Nb pressure tubes. The source of these stresses was either the process used to join the pressure tube to the ends of its fuel channel [5] or from tube straightening [6]. Several examples show that fuel cladding made from Zircaloy is also not immune from DHC. In some Zircaloy nuclear fuel cladding used in boiling-water reactors (BWR), hydride cracking was strongly implicated in long splits that allowed substantial leakage of fission products [7–9]. If the cladding wall is penetrated during operation, for example, by fretting, water from the heat-transport system can enter the fuel cavity where, because of the lower pressure, steam is produced. Much hydrogen is generated because the steam oxidizes the fuel and the inside surface of the cladding, reducing the partial pressure of oxygen and leaving a gas rich in hydrogen. This process is called "oxygen starvation." At some distance from the primary defect, the gas stream becomes almost pure hydrogen, and with breakdown of the protective oxide layer, copious quantities of hydrogen may be absorbed by the cladding [10]. Sometimes, "sunbursts" of hydride formed on the inside surface. With fuel

expansion during fuel rearrangement, the hydrided cladding was stressed, which led to crack initiation. The cracks grew through-wall, propagated axially, and could be over 1 m long. Brittle regions in "chevrons" characterized the fractures, with the crack being longer on the outside surface than the inside surface of the cladding [11]. The lower bounds of the crack velocities were in the range 2.5×10^{-7}–6.6×10^{-7} m/s based on assuming constant growth rates in the time between first detection of the defect and removal of the fuel. The mechanism of cracking appeared to be a form of DHC [8,12], perhaps exacerbated by a continuous additional supply of hydrogen from the steam inside the fuel element [13,14]. A DHC-type of mechanism has been identified as being responsible for radial cracking starting at the outside surface of BWR fuel cladding when power ramped after a high burn-up [15]. Tests on unirradiated cladding demonstrated that the velocity of DHC in the radial direction of the tube obeyed Eq 1, and V was about 10^{-7} m/s at 275°C [16,17]. Cracks in the axial direction, about 20 mm long and close to the end-plugs of Canada Deuterium Uranium (CANDU) fuel, have been detected [18]. The burn-up was very low, 0.4 GWd/t, so the inventory of fission products would be too small to cause stress-corrosion cracking. Several partial radial cracks had also started from the inside surface. The hydrogen concentration was 42 ppm, which may have been picked up from residual moisture in the fuel. The source of the large hoop stress driving the crack was attributed to fuel expansion from the fuel operating well outside its design power, although the cause of this anomaly was not identified.

The two technologically important quantities for DHC are the conditions for crack initiation, K_{IH}, and the rate of crack propagation, V. The latter was the subject of the first part of this International Atomic Energy Agency (IAEA) coordinated research program (CRP) on Zr–2.5Nb pressure tube material [19]. As an extension of this CRP, the rate of DHC has been measured in Zircaloy-4 fuel cladding.

Several methods are available to test fuel cladding for DHC. The first such successful testing was obtained using a center-cracked half-tube loaded in tension [20]. To gain insight on the long splits, tubing containing a central axial crack was loaded by a wedge and mandrel—the SPLIT test [13]. The radial crack propagation from the outside surface has been studied by internally pressurizing tubes containing small axial cracks [16,17]. Axial crack propagation has been measured using the pin-loading tension (PLT) technique [21]. This last method was originally developed at Studsvik for fracture toughness evaluation of thin walled tubing [22,23] and was chosen for the CRP program because

- Its loading is similar to that in a compact toughness specimen used for Zr–2.5Nb;
- In a comparison of test methods for fracture toughness of Zircaloy-4 fuel cladding, the PLT technique provided the lowest values of $J_{0.2}$ and dJ/da, indicating that this technique provides good constraint and limits plasticity at the crack tip [24]; and
- The technique was thought to be amenable to technology transfer.

The IAEA set up this extension to the CRP with the objective of transferring "know-how" on laboratory practices to the member states who were unfamiliar with DHC testing of fuel cladding using the PLT method. The first objective of the program was to establish a uniform and consistent laboratory practice to determine the DHC velocity in the axial direction of fuel cladding so that a meaningful inter-laboratory comparison of the results could be made. A preliminary evaluation showed that the technology transfer was successful [25]. The data from this first trial are included here for completeness. Using six versions of Zircaloy-4 fuel cladding, the second objective was to examine the effects of microstructure on V.

Experimental Details

Test Materials

The material used for the first trial was standard light water reactor (LWR) Zircaloy-4 cladding from Sandvik Lot 86080 [25]. For comparison with this initial trial, samples from Sandvik Lot 83786 were obtained in the cold-worked (CW) condition. During fabrication the final pilgering imposed 80 % CW based on area reduction on a cylindrical mandrel. The dimensions of the tubing are given in Table 1, and the chemical composition is given in Table 2; this material had a slightly higher concentration of oxygen than Lot 86080. The material was tested in the CW condition. Sections of tubing were also heat-treated to simulate that used for pressurized water reactors—CW and stress relieved (CWSR) 480°C for 3.5 h—and for BWRs—recrystallized annealed (RXA) 565°C for 1.5 h. The initial CW microstructure consisted of elongated grains that were little changed by the stress-relieving treatment but completely recrystallized by

TABLE 1—*Dimensions of test materials.*

	Materials				
Dimensions	LWR Sandvik Lot 86080	LWR Sandvik Lot 83786	CANDU Zircatec Lot 226289	CANDU Sandvik Lot 81101	Atucha FAE Lot MA-61
Outside diameter, D (mm)	9.5	9.5	13.1	13.1	11.9
Wall thickness, t (mm)	0.57	0.60	0.39	0.39	0.55
D/t	16.7	15.8	33.6	33.6	21.6

the higher temperature anneal, with grains that were almost equiaxed having a mean diameter of about 3 μm. The basal plane normals were concentrated about 30° from the radial direction; the texture factors, F, in the three principal directions—radial, R; transverse, T; and axial, A—are summarized in Table 3. The basal plane normals rotated a small amount from the radial direction toward the transverse direction with heat-treatment. The ultimate tensile strength (UTS) was measured with ring tensile tests; it was reduced by heat-treatment and test temperature, Table 4.

Three other batches of cladding were tested. For the CANDU cladding supplied by Zircatec, the last stage of cold-working was about 90 %, and the final stress relieving was 500°C for 8 h. The composition of the Zircaloy-4, Table 2, and the (0002) distribution Table 3, were similar to those of the LWR cladding. The dimensions of the CANDU cladding differ from the LWR cladding having a larger diameter and thinner wall, Table 1. It also has lower strength, Table 4. The clearly defined grains were elongated in the axial direction but almost equiaxed on the transverse-radial section with a mean grain diameter of about 4 μm. For the CANDU cladding supplied by Sandvik, the composition of the Zircaloy-4 is given in Table 2. This CANDU cladding also differs from the LWR cladding having a larger diameter and thinner wall, Table 2, and lower strength, Table 4. The grain size was about 5.8 μm on the transverse-radial section but elongated in the longitudinal direction. For the Atucha cladding, the last stage of cold-working was 57 %, and the final stress relieving was 510°C for 8.5 h. The composition of the Zircaloy-4, Table 2, and the (0002) distribution, Table 3, again were similar to those of the LWR cladding. The Atucha cladding had a larger diameter but similar wall thickness as the LWR cladding, Table 1, and lower strength, Table 4. The

TABLE 2—*Chemical composition of test materials.*

	Materials				
Element	LWR Sandvik Lot 86080	LWR Sandvik Lot 83786	CANDU Zircatec Lot 226289	CANDU Sandvik Lot 81101	Atucha FAE Lot MA-61
Sn (wt %)	1.25	1.26	1.3	1.35	1.29
Fe (wt %)	0.22	0.23	0.22	0.22	0.23
Cr (wt %)	0.1	0.12	0.12	0.10	0.12
O (ppm)	1180	1272	1180	1260	1200
Si (ppm)	100	100	100	60	98
C (ppm)	120	120	140	120	132
N (ppm)	49	41	24	<30	28
H (ppm)	7	7	8	13	4

TABLE 3—*Texture factors for basal planes in test materials.*

	Materials					
Texture Factors	LWR Sandvik Lot 86080 CWSR	LWR Sandvik Lot 83786 CW	LWR Sandvik Lot 83786 CWSR	LWR Sandvik Lot 83786 RXA	CANDU Zircatec Lot 226289	Atucha FAE Lot MA-61
F_R	0.65	0.65	0.64	0.60	0.65	0.56
F_T	0.30	0.29	0.31	0.34	0.30	0.29
F_L	0.05	0.06	0.05	0.06	0.05	0.15

TABLE 4—*Tensile properties of test materials.*

Material	Test Temperature (°C)	UTS (MPa)
Sandvik, Lot 86080, CWSR	200	543
	250	502
	290	477
	320	459
Sandvik, Lot 83786, CW	200	588
	250	532
	290	498
	320	475
Sandvik, Lot 83786, CWSR, 480°C for 3.5 h	200	570
	250	510
	290	489
	320	466
Sandvik, Lot 83786, RXA, 565°C for 1.5 h	25	517
	250	270
	350	228
CANDU, Zircatec, Lot 226289, 500°C for 8 h	22	606
	100	509
	200	415
	300	370
	350	346
CANDU, Sandvik, Lot 81101	20	589
	250	424
Atucha, FAE, Lot MA-61	20	575
	200	406
	250	367
	300	346

clearly defined grains were elongated in the axial direction but almost equiaxed on the transverse-radial section, with a mean grain diameter of about 2 μm in the radial direction and 3 μm in the transverse direction.

Specimen and Fixture Preparation

After cleaning the cladding, a layer of hydride was deposited on the surfaces electrolytically using 0.1*M* H_2SO_4, a temperature of 65 ± 5°C, and a current density of 1 kA/m^2. Diffusing the hydrogen into the metal by annealing at 410°C for 24 h added a homogeneous hydrogen concentration of about 200 ppm. The resulting hydrides had their plate normal in the radial direction. The hydrogen concentration was confirmed by analysis using an inert gas fusion technique. For a few specimens the hydrogen was added gaseously at 400°C, with similar results.

The test specimen is shown Fig. 2. The 13 mm long specimen (c_A) contained diametrally opposite axial notches at both edges with those at one end being sharpened by fatigue at room temperature for a

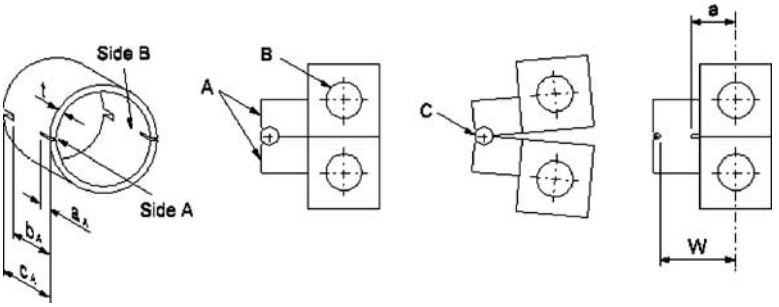

FIG. 2—*Schematic diagram of test specimen and PLT fixture.*

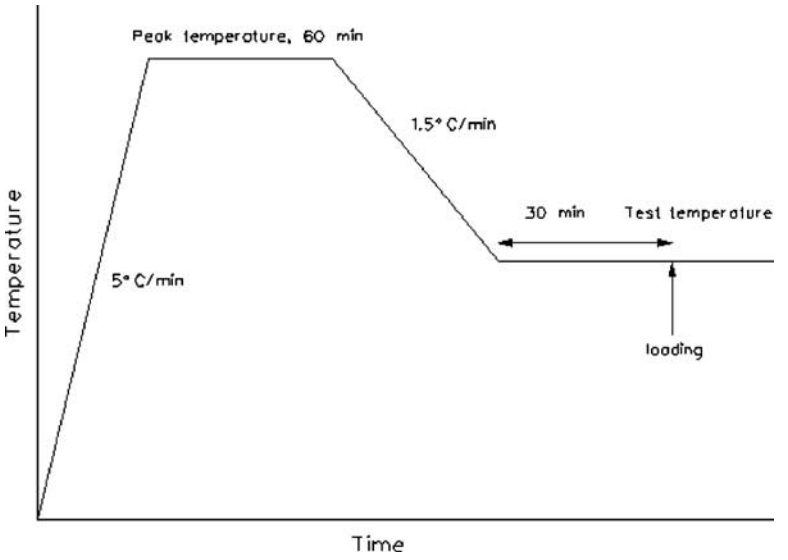

FIG. 3—*Schematic diagram of temperature cycle used for DHC tests.*

starting length of a_A; the notch at the other end provided an effective specimen length of b_A. The notch that was fatigued to a crack was 0.15 mm wide, while the rear notch was 0.5 mm wide. The fatigue pre-cracking was done at 1–5 Hz with starting maximum loads of 200–300 N cycled down to 50 N. The maximum load was gradually reduced to 90–100 N as the crack progressed. The final load was chosen to be lower than the starting load for the DHC test, typically 160 N, so the plastic zone at the crack tip from fatigue did not interfere with DHC. Between 8000 and 50 000 cycles were required to produce a suitable starting crack, about 1.5 mm in length. The crack length was measured either visually on the surface or using potential drop (PD).

The PLT fixture is shown schematically in Fig. 2. Most of the fixtures were made from Nimonic 90, but successful testing has been achieved using fixtures made from carbon steel. The fixture consisted of two halves, which, when placed together, form a cylindrical holder, A. The diameter of the holder allowed it to be inserted into the specimen while maintaining a small gap. The fixture halves were loaded in tension through pins at B and rotated about a pin C at the ends of the cylindrical holder providing similarity to the loading of a compact toughness specimen but on two cracks. Care was taken to line up the pre-cracked notches with the join of the two halves of the fixture.

Delayed Hydride Cracking Testing

To start a DHC test, the specimen was heated to and held at a temperature of 50–75 °C above the test temperature for 1 h, then cooled with no undercooling to the test temperature. This temperature history encourages cracking and minimizes variation; this sequence represents T_4 to below T_6 in Fig. 1 rather than T_1 to T_3 in Fig. 1, where cracking can be difficult. After a short period at constant temperature, at least 30 min, the specimen was loaded to a K_I of about 15 MPa$\sqrt{}$m. The test history is depicted in Fig. 3. The value of K_I was calculated from Eq 2

$$K_I = [P/(2t\sqrt{W})]f(a/W) \tag{2}$$

where:

P=load (N),

t=wall thickness of the cladding (m),

W=effective width of specimen (m), being the distance from the load line to the axis of rotation (see Fig. 2),

a=effective crack length (m), being the distance from load line to the crack tip (see Fig. 2), and

$f(a/W)$=geometry correction factor.

The value of $f(a/W)$ was determined experimentally from compliance measurements, resulting in

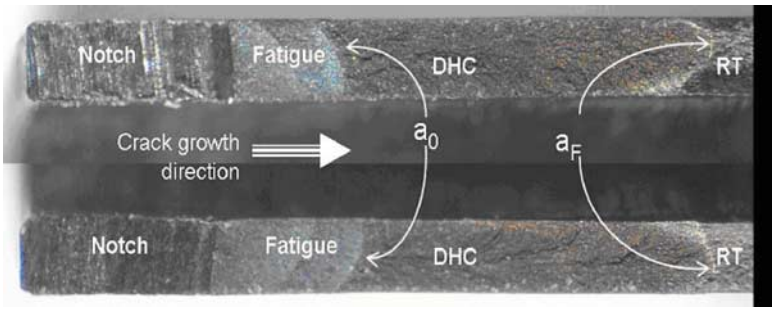

FIG. 4—*View of the fracture surfaces of CWSR Zircaloy-4 specimen (200 ppm of hydrogen). The top and bottom edges are the outside surfaces of the cladding. The initial (a_0) and the final (a_F) lengths of the DHC crack are indicated as well as the areas of notch, fatigue pre-cracking, DHC crack propagation, and room temperature fracture after the DHC test (RT). The cladding wall thickness is 0.57 mm.*

$$f(a/W) = 92.203 - 468.73(a/W) + 787.15(a/W)^2 - 360.99(a/W)^3 \quad (3)$$

for LWR cladding [26] and

$$f(a/W) = -0.4759 + 13.185(a/W) + 39.533(a/W)^2 - 23.65(a/W)^3 + 12.135(a/W)^4 - 2.9162(a/W)^5 \quad (4)$$

for CANDU cladding [27].

Cracking was detected either by PD or by displacement equivalent to crack opening. Once the cracks had extended 2–3 mm, the load was removed and the specimen was cooled to room temperature. The crack surfaces were lightly heat-tinted from oxidation, and the ends of the crack could usually be discerned on the fracture surface. An alternative was to briefly fatigue the specimen to mark the end of the DHC. Subsequently, the specimen was broken open, and the fracture surface was examined. A typical pair of fracture surfaces is shown in Fig. 4. In this example the delayed hydride crack is about 3 mm long. Crack growth by DHC, $a_F - a_0$ (Fig. 4), was estimated on each crack from the average of nine equally spaced measurements; the value for the specimen, a_S, was the average of the values of the two cracks. Often an incubation period, t_i, was required before DHC started; cracking time, t_T, was taken as (time under load—t_i). Crack velocity, V, in the axial direction of the cladding was a_S/t_T. Scanning electron microscopes were used to examine the fracture surfaces of some specimens to provide details of the fracture mechanism. Cracking was evaluated in the temperature range of 144–302°C.

All the testing and examinations were performed in the ten laboratories listed with the authors' names.

Results

Fracture Surfaces

The periods of the different fracture modes were not only distinguishable by oxidation, Fig. 4, but the microfractographic features were different. The pre-fatigue region contained typical striations formed at room temperature and subsequently oxidized during DHC testing, Fig. 5. DHC is shown in Fig. 6 as areas of flat fracture corresponding to cracked hydrides, interspersed by curved features that correspond to changes in crack plane or direction. The interface between fatigue and DHC, Fig. 7, or DHC and ductile fracture, Fig. 8, were easily distinguished along *A-A*. The post-test stage of the fracture surface consisted of ductile fracture formed when the specimen was broken open at room temperature; the large fissures between the areas of ductile dimples are probably fractured circumferential hydrides that are perpendicular to the fracture plane, Fig. 8. Fractographs of the materials in all metallurgical states showed the same features. To date, the DHC striations usually seen in Zr–2.5Nb, Fig. 9(*a*), have been observed only once, Fig. 9(*b*). This specimen was CWSR Zircaloy-4 cladding, and the striations were in the high K_I region, between about 25 and 40 MPa$\sqrt{}$m. This specimen had been subjected to 12 temperature cycles between 248 and 270°C. The cladding made from Zr–2.5Nb was in the CWSR condition and tested at 250°C; the striations were very similar to those observed on the DHC fracture surfaces of Zr–2.5Nb pressure tube materials [19].

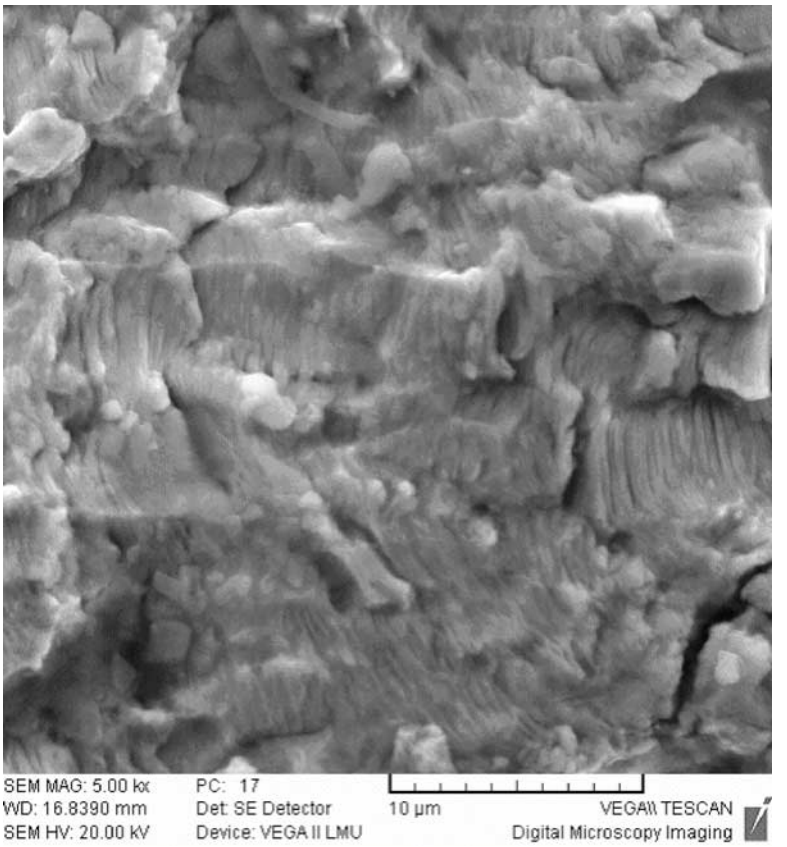

FIG. 5—*Fatigue striations formed at room temperature on specimen of CANDU Zircaloy-4 fuel cladding tested at 250°C.*

Incubation Times

The time before continuous DHC started was very variable in all the materials. At test temperatures below 280°C, some specimens appeared to start cracking immediately on application of the load, whereas others required considerable time before cracking started. Factors contributing to the variability in the start of DHC are the sensitivity of the crack detection system and the variation in the preparation of the starter-crack by fatigue. In all materials except RXA, the incubation time had mean values between 3 % and 7 % of the test time; thus errors in their determination contributed only a small error to the value of crack velocity. Unlike with Zr–2.5Nb [19], no temperature dependence of the incubation time could be discerned.

Crack Velocities

The initial value of K_I depends on the load and the crack length after fatigue. The load is well known, but the initial crack length has some variation because it is difficult to measure accurately before the DHC test. For these tests the target for the initial value of K_I was 15 $\text{MPa}\sqrt{\text{m}}$. In practice it varied between 11.0 and 25.0 $\text{MPa}\sqrt{\text{m}}$, but the mean value for all the tests was 16.4 $\text{MPa}\sqrt{\text{m}}$, close to the target, with a moderate dispersion of 3.0 $\text{MPa}\sqrt{\text{m}}$. Most laboratories obtained seemingly valid results with amounts of crack growth varying from 0.4 to 4.2 mm; the mean value for all the tests on LWR CW and CWSR materials was 2.0 ± 0.86 mm. Consequently the final value of K_I had a wide range, up to 43 $\text{MPa}\sqrt{\text{m}}$. One expects that V should be independent of either initial or final K_I (so long as K_{IH} is exceeded) and therefore crack length, and the results confirm this expectation. For example, Fig. 10 shows the lack of dependence of the crack velocity on amount of crack growth in CWSR material at 250°C.

The temperature dependence of V for the CW and CWSR materials is depicted in Fig. 11. Below about 280°C the velocity followed Eq 1, with Q around 55 kJ/mol. Above 280°C, V was very scattered and declined until cracking was absent at 295°C. (In tests at high temperature where no cracking was observed, the plotted value was obtained by dividing an assumed crack propagation of 0.01 mm by the test

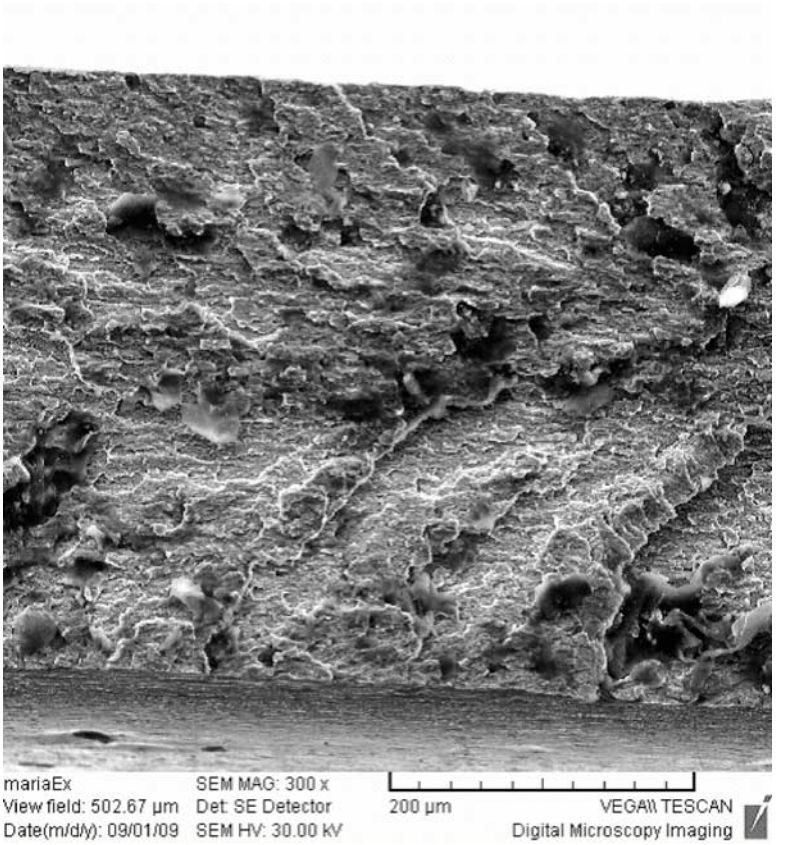

FIG. 6—*DHC in CANDU Zircaloy tested at 250°C. Cracking from right to left.*

time.) The behavior of the RXA material was quite different—often cracking was reluctant to start, and when it was observed, its rate was very scattered, Fig. 12, making evaluation of any temperature dependence unclear. (Using an upper bound line of the data may indicate similar temperature dependence to that of the other cladding, but such a treatment is difficult to justify with the current large variation.) The number of tests on the non-LWR materials was only sufficient to obtain general trends, Fig. 13. The CANDU Zircatec and Atucha materials had similar values of V and showed the now-expected drop at high test temperatures. The CANDU Sandvik cladding cracked faster than the other two materials; it only provided a hint of decline at the highest test temperature, 295°C, since V was similar to that at 250°C.

Discussion

For both batches of LWR cladding in the CWSR condition, the values of V and their temperature dependence were in very good agreement, Fig. 14, showing that the testing technique was under control and reproducible. Compared with CWSR material, the CW material had similar temperature dependence, but slightly higher values of crack velocity (below 275°C the average value was about a factor of 1.5 higher) and maybe a slightly higher temperature for the start of the decline in V, 285 versus 275°C, Fig. 11.

In the usual picture of DHC, after K_{IH} is exceeded, the crack velocity is almost independent of K_I and crack length. The crack velocity at 250°C of CWSR material was insensitive to crack length, Fig. 10, and therefore K_I over a wide range of values. The implication is that K_{IH} for this material was lower than 11 MPa$\sqrt{m}$, the lowest value tested at which cracking was observed. The results on RXA material at 250°C indicate that the crack velocity was highly K_I-dependent in this condition, Fig. 15, suggesting that K_{IH} is large for this material, perhaps as high as 25 MPa$\sqrt{m}$. (In this figure K_I is taken as (initial value +final value)/2.) This high sensitivity to K_I also explains the large variation in values of V obtained in this material and frequent difficulty with initiating cracking.

The mean values of V for CW and CWSR materials from this study were higher than those from measurements on pressure tubes made from Zircaloy-2 [28,29], Fig. 16, but similar to the few measurements on Zircaloy-4 fuel cladding [16,20,21], suggesting similar temperature dependence, independent of

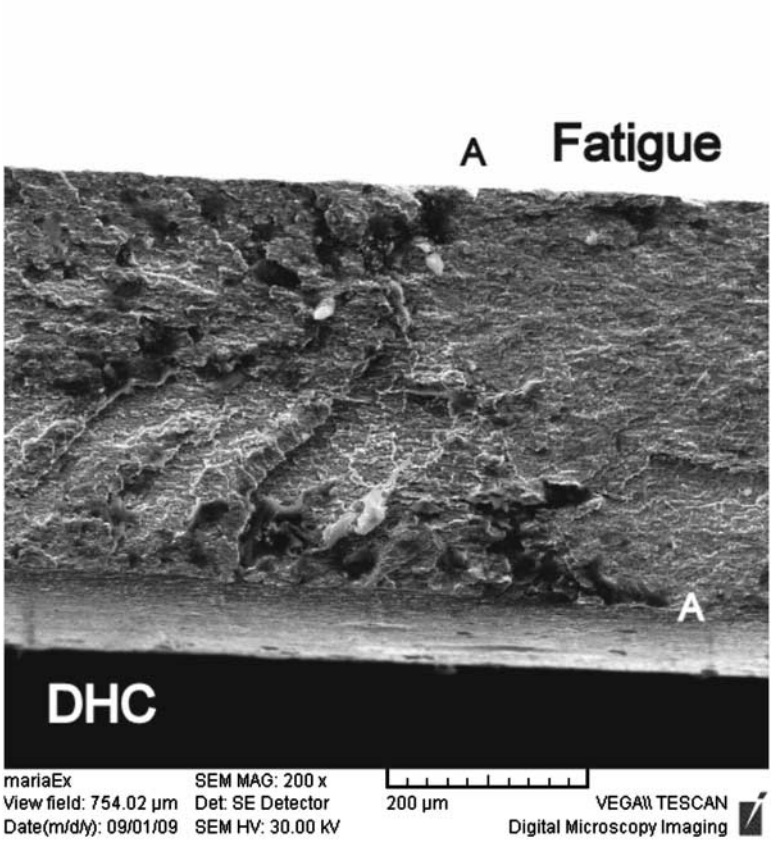

FIG. 7—*Interface between fatigue pre-crack and DHC in CANDU Zircaloy tested at 250°C. Cracking from right to left.*

test direction on the plane perpendicular to the hoop stress, Fig. 17. The variability in values can be attributed to

- Differences in the histories of temperature can contribute large variations in crack velocity through the behavior illustrated in Fig. 1,

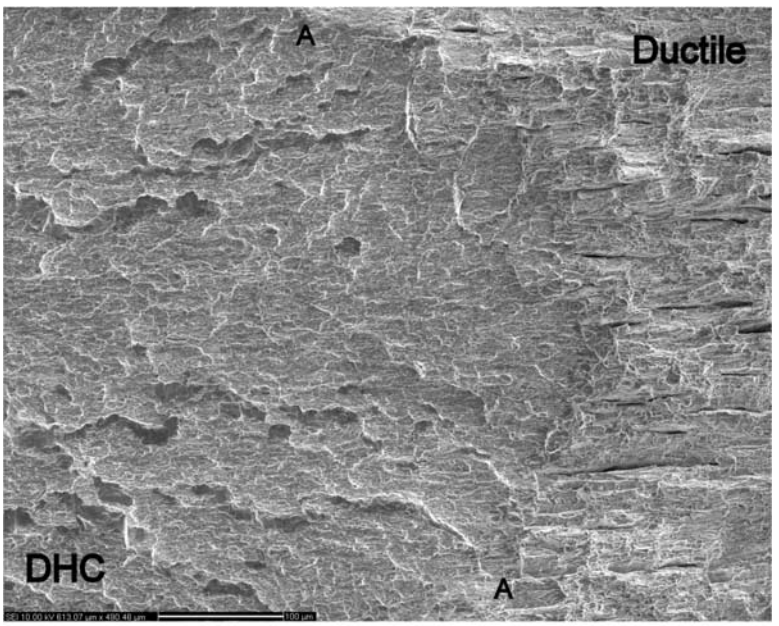

FIG. 8—*Interface between DHC at 144°C and ductile fracture at 25°C after DHC test. CWSR Zircaloy-4 fuel cladding. Cracking from left to right.*

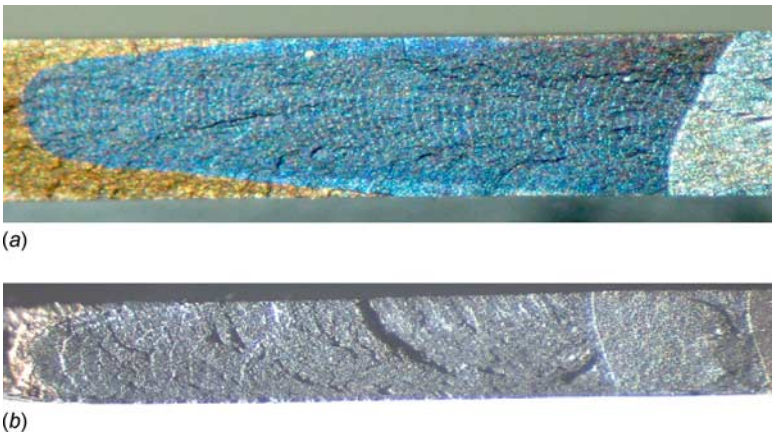

FIG. 9—*Striations observed on (a) CWSR Zr–2.5Nb cladding tested at 250°C and (b) on one specimen of CWSR Zircaloy-4 during DHC with thermal cycles.*

- The small number of samples tested; the process of DHC is highly variable and even in well-controlled testing, the crack velocity in fuel cladding can vary by a factor of about three [25] (small numbers of specimens may lead to large variations in apparent temperature dependence), and
- Differences in microstructure, including texture, and strength.

In Zr–2.5Nb [30] and Zircaloy-2 pressure tubes [28], the crack velocity and K_{IH} are very sensitive to testing direction and cracking plane. This behavior is attributed to crystallographic texture. In pressure tubes in the CW condition, the basal plane normals are strongly oriented in the transverse direction. Cracking in the axial direction driven by a hoop stress is much faster and requires a much lower K_{IH} than cracking in the circumferential direction driven by an axial stress. The explanation is that hydrides reorient readily from the circumferential orientation to the radial direction with a hoop stress but not with an axial stress because the normal to the basal planes of the zirconium crystals, which are close to the habit planes of hydride, are parallel with the hoop direction and not the axial direction. A radial texture has been proposed to protect Zr–2.5Nb from DHC [31,32]. In all the fuel cladding tested in this study, the texture was highly radial, Table 3, yet DHC was observed at velocities slightly higher than in pressure tube materials with transverse textures. The threshold tensile stress to start reorienting hydrides in Zircaloy-4 fuel cladding is low—typical values are 120 MPa for CWSR cladding and 70 MPa for RXA cladding

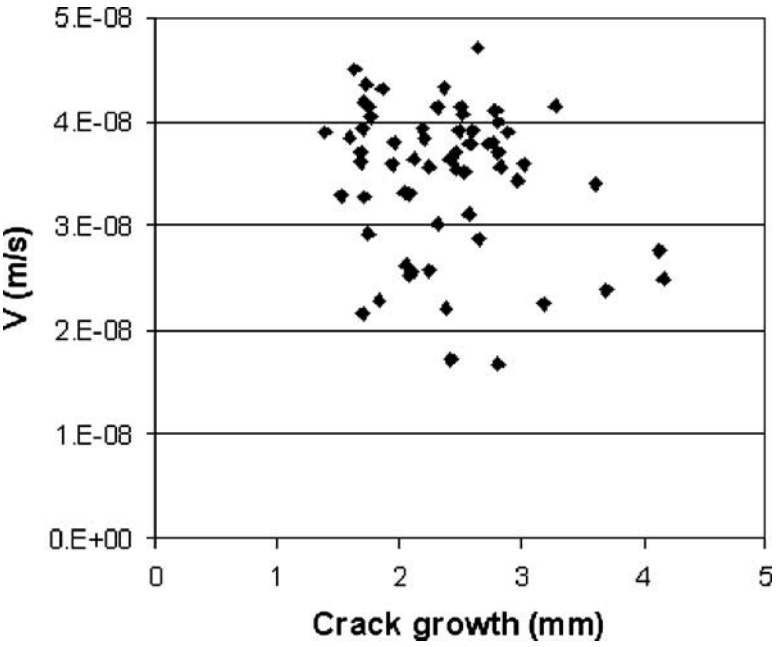

FIG. 10—*No dependence of V on crack length; CWSR material tested at 250°C. (Data from Ref 25 and this paper.)*

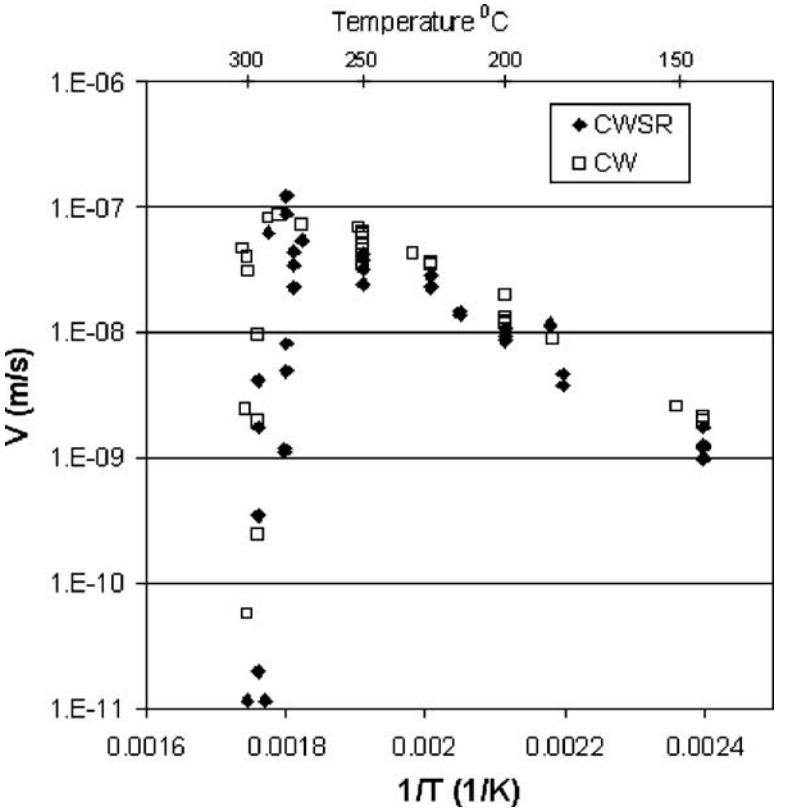

FIG. 11—*Temperature dependence of V in Zircaloy-4 fuel cladding in the CW and CWSR conditions.*

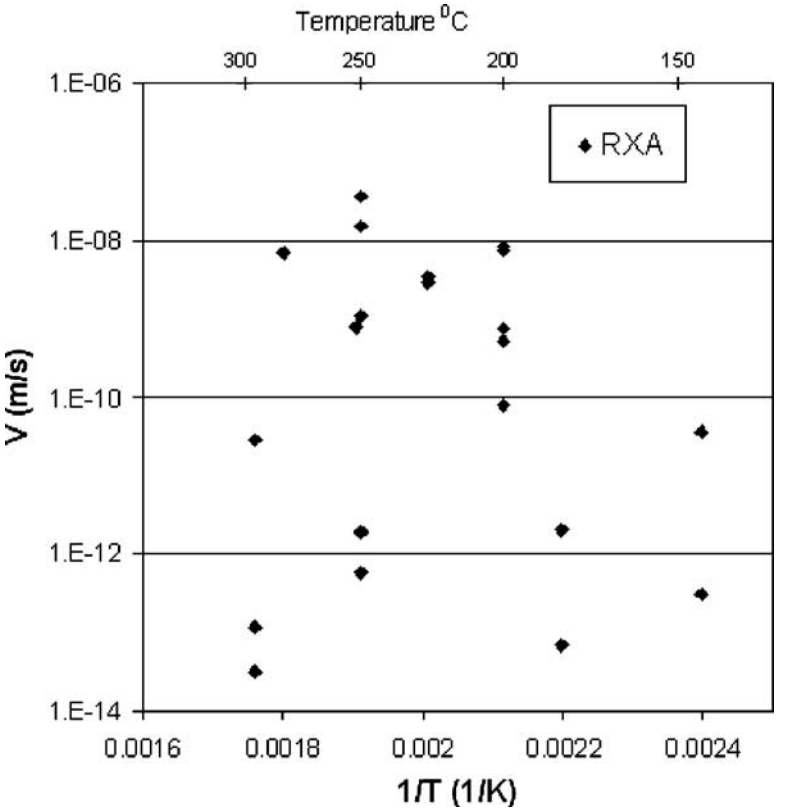

FIG. 12—*Temperature independence of V in Zircaloy-4 fuel cladding in the RXA condition.*

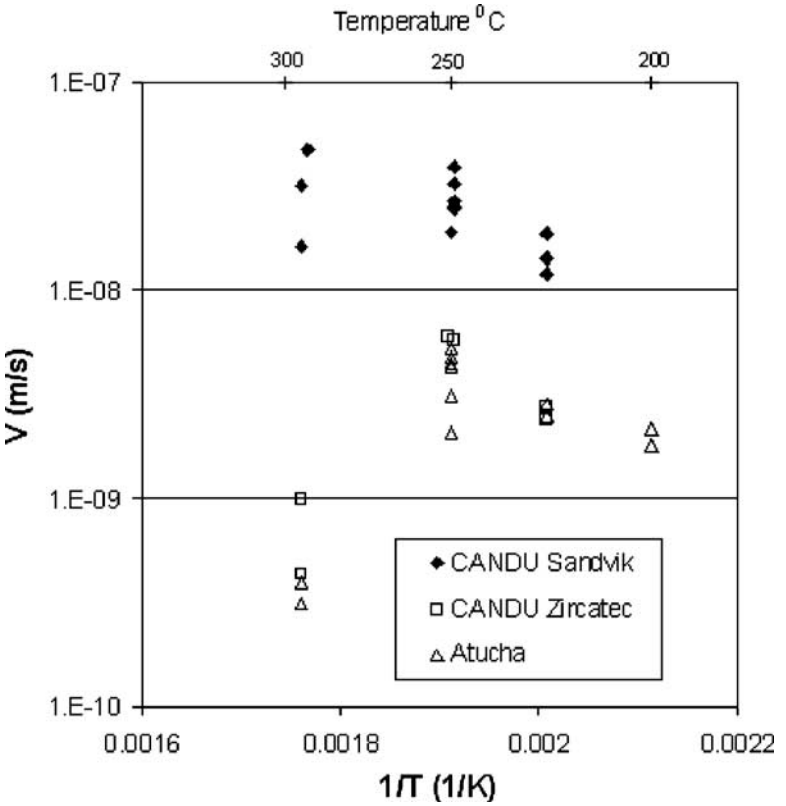

FIG. 13—*Temperature dependence of V in Zircaloy-4 fuel cladding representing CANDU, from Zircatec and Sandvik, and Atucha.*

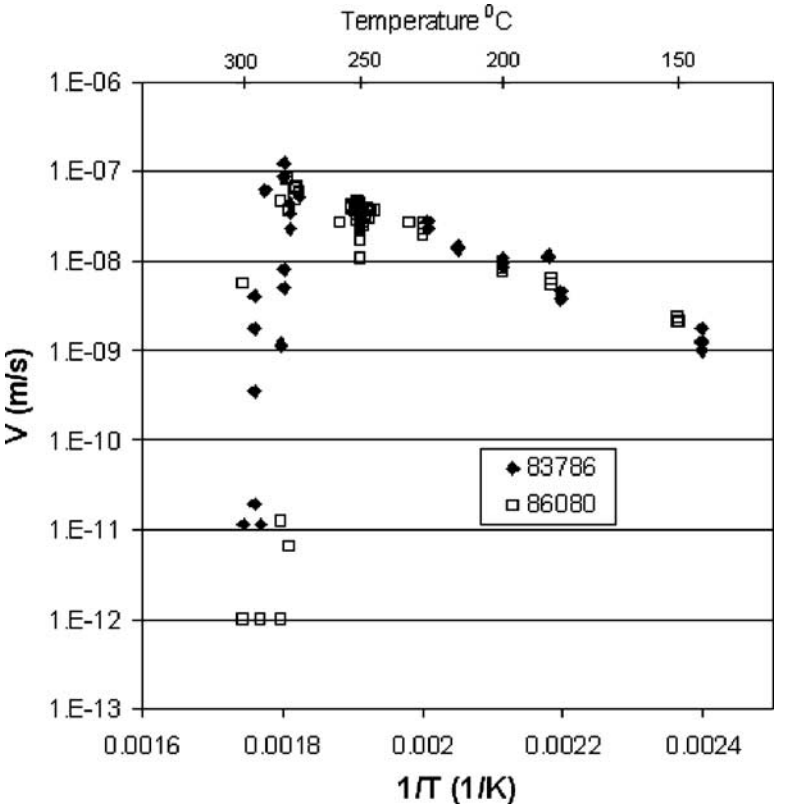

FIG. 14—*Comparison of DHC behavior of LWR Zircaloy-4 fuel cladding in the CWSR condition; data for Lot 86080 from Ref 25.*

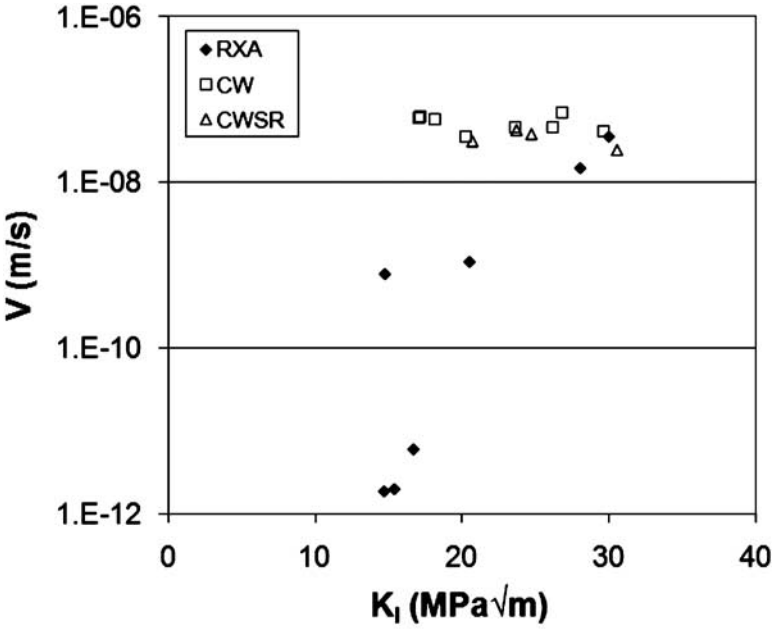

FIG. 15—*K_I dependence of V at 250°C for Zircaloy-4 fuel cladding in three metallurgical conditions.*

[33]—so difficulty in reorienting hydrides does not provide an impediment for DHC in cladding since the tensile stresses at the crack tip exceed the threshold stresses for hydride reorientation.

The value of DHC velocity is dominated by the diffusivity and the solubility limits of hydrogen in the zirconium alloy and to a lesser extent by the strength. Zircaloy-4 is essentially a single-phase alloy, with a distribution of intermetallic particles, and, with little error, the heat-treatments should not affect the diffusivity or solubility limits. Although yield strength would be the preferred over UTS as the strength

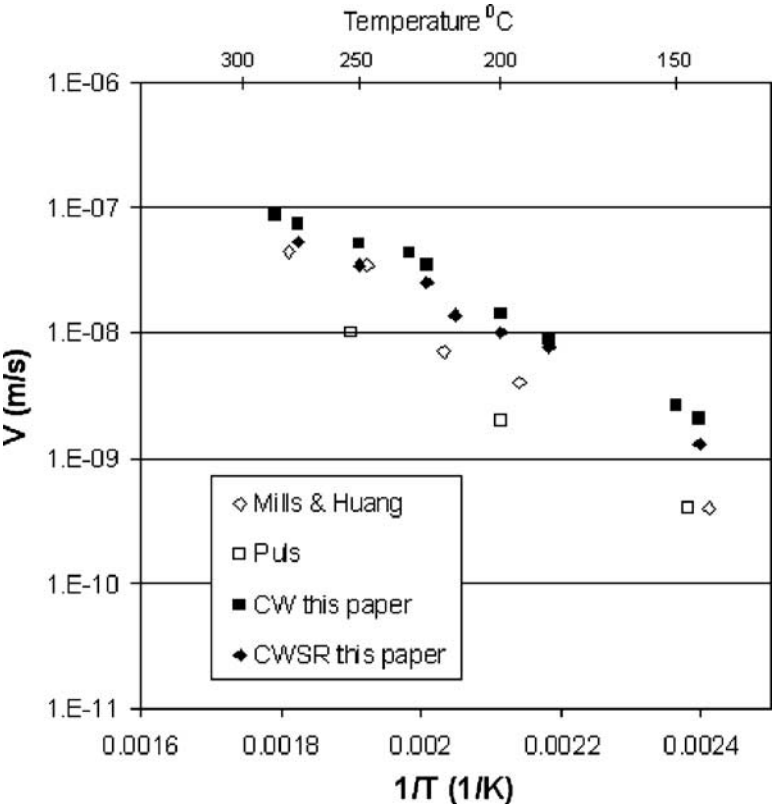

FIG. 16—*Comparison of temperature dependence of DHC in Zircaloy-2 pressure tubes [28,29] and Zircaloy-4 fuel cladding [this paper] up to 280°C.*

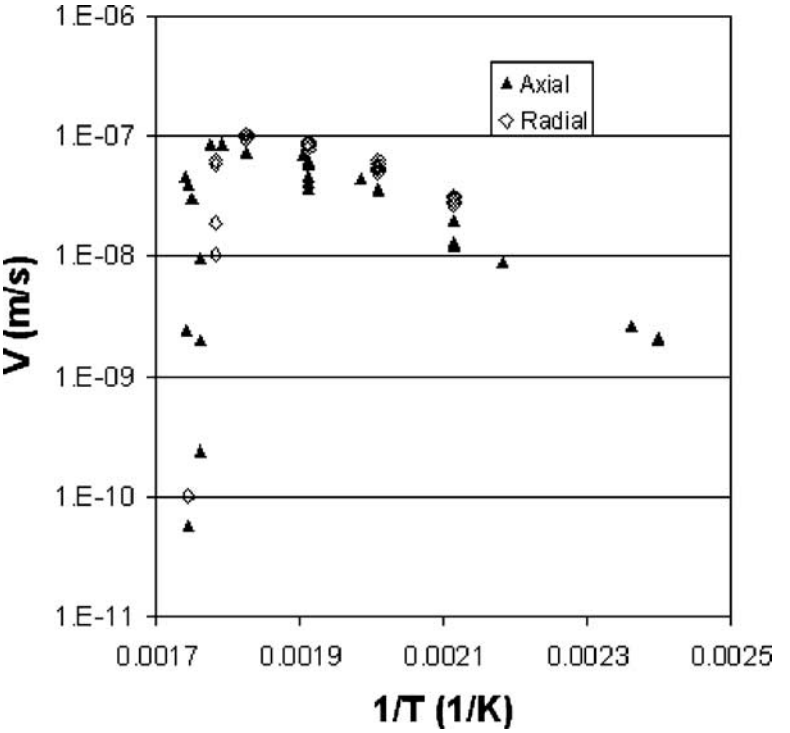

FIG. 17—*Comparison of temperature dependence of cracking in axial (this paper) and radial [16] directions in CW Zircaloy-4 fuel cladding.*

variable for fracture analysis, only the latter values were available. Comparing V at a single temperature can be used to evaluate the effect of strength on V. A modest correlation ($R^2=0.84$) is found between UTS and the mean value of V at 250°C for the current batches of fuel cladding, except the RXA material, Fig. 18. The RXA material was excluded from the linear fit, but it was included in the figure for completeness and to emphasize how its behavior was different from that of the other tubing. The CANDU Sandvik cladding was stronger than the other two non-LWR claddings, and its higher value of V reflects this added strength. Values from Zircaloy-2 pressure tubes are in general agreement with those for fuel cladding, indicating that it is strength rather than texture that is causing the difference in values shown in Fig. 16.

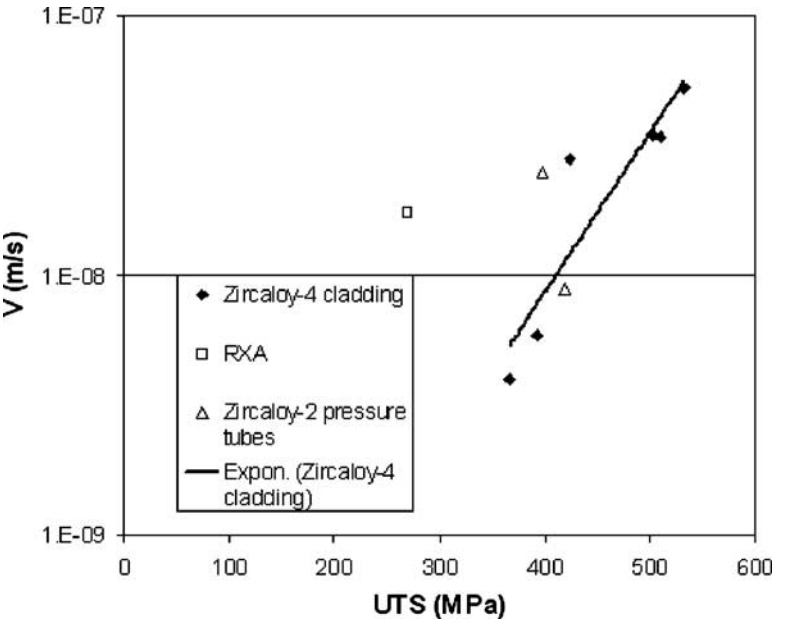

FIG. 18—*Effect of strength on mean DHC velocity in Zircaloy at 250°C.*

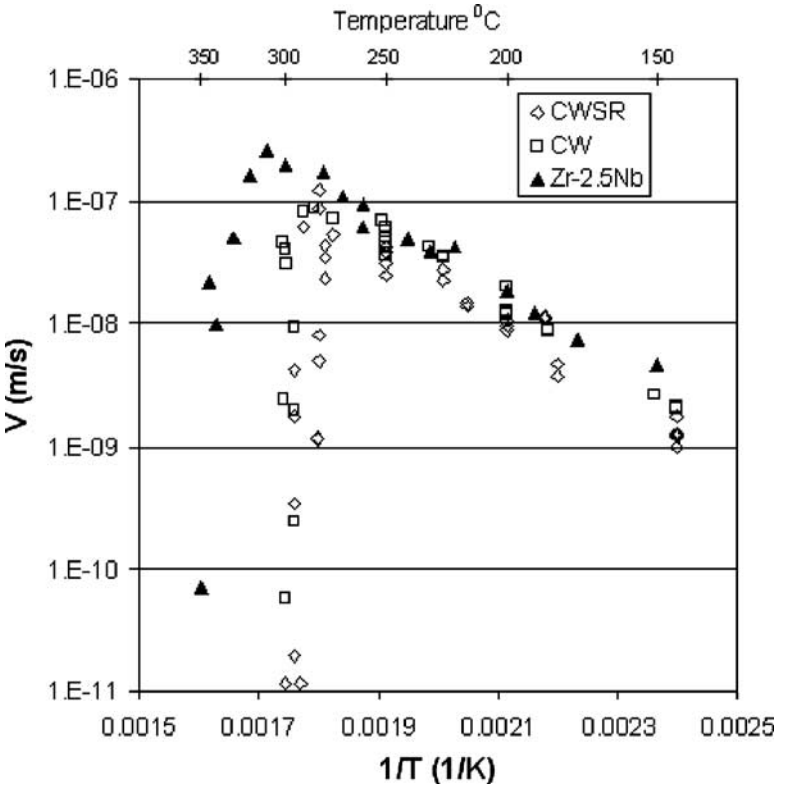

FIG. 19—*Comparison of decline in DHC at high test temperatures in CW Zr–2.5Nb [34] and CW and CWSR Zircaloy-4 fuel cladding [this paper].*

In this study, the fracture surfaces attributed to DHC were clearly distinct from those made by fatigue or ductile rupture. As previously observed with Zircaloy [20,21,28], the fractographic features called striations were absent, with one exception, Fig. 9(*b*). These observations are in marked contrast to the fractography of Zr–2.5Nb where striations are easily and commonly observed, Fig. 9(*a*). Striations are bands across most of the width of a specimen, perpendicular to the crack growth direction, consisting of regions of ductile fracture bounding cleavage of hydride. They tend to remain almost a constant width and coplanar as the crack extends. In Zircaloy, the hydrides fracture on different planes along the crack front with ductile fracture between the brittle plates. The size of the brittle areas is variable, so bands of consistent width are not formed. This observation supports the idea that the microstructural features contributing to the difference in behavior of the two materials are probably the fine scale of the grains and the presence of a β-phase in Zr–2.5Nb. The single observation of striations in Zircaloy-4 may be linked to the thermal cycles imposed during the test where each striation corresponded to the stopping and restarting of cracking. The general lack of striations with DHC in Zircaloy in isothermal tests suggests that they are not a fundamental characteristic of DHC.

The decline of DHC at high temperatures has been observed in both Zr–2.5Nb [3,34,35] and Zircaloy [36]. This feature is apparent in each of the cladding materials tested, except for the RXA material where the scatter obscures any temperature dependence. As an example, Fig. 19 is a comparison of the behavior of CW Zr–2.5Nb pressure tube material [34] and Zircaloy-4 fuel cladding in the CW and CWSR conditions. In Zr–2.5Nb the crack velocity starts to deviate from the Arrhenius correlation at about 310°C with no cracking detected at 350°C, while in the current Zircaloy-4 the initial deviation is between 275 and 285°C with no cracking at 300°C.

The rate of DHC can be suppressed when

- The hydrogen concentration is insufficient for hydrides to form at the crack tip (the current specimens contained 200 ppm hydrogen, which is sufficient for hydrides to be present at temperatures up to 360°C even on cooling to the test temperature; thus the observed reduced rate of cracking is not caused by lack of hydride),
- the temperature history prevents hydrides from forming at the crack tip (heating to the test temperatures may cause this situation even if hydrides are present in the metal matrix [37]; in the

current tests the test temperature was always attained by cooling from at least 50°C above the test temperature with no undercooling, so this effect is not the cause of the reduced velocity), and

- K_{IH} is greater than the applied K_I. (In Zr–2.5Nb, K_{IH} has little temperature dependence at temperatures below 300°C, but at higher temperatures it increases rapidly [35]. Zircaloy-4 likely behaves in a similar manner, implying that K_{IH} increases to values greater than 16 $MPa\sqrt{m}$ above 280°C.) A corollary to this behavior is that V and the crack suppression temperature will appear to depend on K_I. Close to the critical temperature, a small amount of evidence supports this conclusion. In Zr–2.5Nb the range of the suppression temperature increased from 280–313 to 328–359°C when K_I was increased from 13 to 17 $MPa\sqrt{m}$ [3]. In the current study, at 283°C in one specimen no cracking was detected after 9000 s at a K_I of 15 $MPa\sqrt{m}$, but once K_I was increased by about 7 %, the crack progressed but at a much reduced rate based on expectations from an extrapolation of Eq 1.

The maximum value of V in this study was 1.2×10^{-7} m/s at 282°C for CWSR material, which is two to six times lower than the rates estimated from splits in LWR cladding [14]. The current results are not suitable for direct application to the behavior of fuel cladding because the material is unirradiated. The added strength generated by irradiation has two consequences: The crack velocity is increased by a factor between three and ten [20,21], easily agreeing with the rates observed in-reactor, and the high temperature decline in velocity is postponed to higher temperatures [35]. Other differences between cladding on an operating fuel element and these laboratory experiments include temperature gradients, which can increase crack velocity and postpone the response of V when the temperature is attained by heating [38,39]. During dry storage of spent fuel, the cladding may reach temperatures of around 400°C. The high temperature limit suggests that failure by DHC should not be possible for several years as the fuel cools toward the temperatures at which cracking may be observed.

Summary

The rate of DHC has been evaluated in Zircaloy-4 fuel cladding in several metallurgical conditions using the PLT technique. At temperatures below about 280°C, the cracking followed an Arrhenius behavior, but at higher temperatures the rate declined with no cracking above 300°C. The main role of microstructure is to control the material strength; the cracking rate increased as the strength increased. The radial texture did not protect the cladding from DHC. In all the cladding, except that in the recrystallized condition, cracking rate was independent of K_I, indicating that K_{IH} was below 11 $MPa\sqrt{m}$. In the recrystallized material the cracking rate was highly variable because it depended on K_I within the test range of up to 25 $MPa\sqrt{m}$. The DHC fracture surface consisted of flat broken hydrides, often in arcs, and, with one exception, no striations were observed.

Acknowledgments

The writers are grateful to the IAEA for financial support. The authors would also like to acknowledge the following technical assistance: A. Buyers, A. Lockley, and Zhang He (Atomic Energy of Canada Limited, CRL) characterized the materials; R. Jakobsson and B. Johansson (Studsvik) and P. Kotov (Bochvar Institute) provided mechanical testing; M. Mihalache (INR) performed fractography; and R. N. Singh and G. Sanyal (BARC) helped with the DHC testing. Zircatec donated CANDU cladding, and CONUAR-FAE donated Atucha cladding.

References

[1] Coleman, C. E., "Cracking of Hydride-Forming Metals and Alloys," *Comprehensive Structural Integrity*, Vol. 6, I. Milne, R. O. Ritchie, and B. Karihaloo, Eds., Elsevier, Kidlington, Oxford, UK, 2003, Chap. 6.03, pp. 103–161.

[2] Cheadle, B. A., Coleman, C. E., and Ambler, J. F. R., "Prevention of Delayed Hydride Cracking in Zirconium Alloys," *Zirconium in the Nuclear Industry—Seventh International Symposium, ASTM STP 939*, Strasbourg, France, June 24–27, 1985, R. B. Adamson and L. F. P. Van Swam, Eds., ASTM

International, West Conshohocken, PA, 1987, pp. 224–240.
[3] Smith, R. R. and Eadie, R. L., "High Temperature Limit for Delayed Hydride Cracking," *Scr. Metall.*, Vol. 22, 1988, pp. 833–836.
[4] Simpson, C. J. and Ells, C. E., "Delayed Hydrogen Embrittlement in Zr–2.5 wt%Nb," *J. Nucl. Mater.*, Vol. 52, 1974, pp. 289–295.
[5] Perryman, E. C. W., "Pickering Pressure Tube Cracking Experience," *Nucl. Energy*, Vol. 17, 1978, pp. 95–105.
[6] Platonov, P. A., Ryazantseva, A. V., Saenko, G. P., Knizhnikov, Y. N., and Viktorov, V. F. "The Study of Cause of Cracking in Zirconium Alloy Channel Tubes," *Poster Paper at ASTM Zirconium in the Nuclear Industry—Eighth International Symposium*, San Diego, CA, June 19–23, 1988, ASTM, Philadelphia, PA, 1988, available as AECL Report RC-87.
[7] Jonsson, A., Hallstadius, L., Grapengiesser, B., and Lysell, G., "Failure of a Barrier Rod in Oskarshamn-3," *Fuel for the '90's, International Topical Meeting on LWR Fuel Performance*, Avignon, France, April 21–24, 1991, American Nuclear Society, La Grange Park, IL and European Nuclear Society, Brussels, Belgium, 1991, pp. 371–377.
[8] Schrire, D., Grapengiesser, B., Hallstadius, L., Lundholm, I., Lysell, G., Frenning, G., Ronnberg, G., and Jonsson, A., "Secondary Defect Behaviour in ABB BWR Fuel," *International Topical Meeting on Light Water Reactor Fuel Performance*, West Palm Beach, April 17–21, 1984, American Nuclear Society, La Grange Park, IL, 1994, pp. 398–409.
[9] Armijo, J. S., "Performance of Failed BWR Fuel," *International Topical Meeting on Light Water Reactor Fuel Performance*, San Diego, CA, June 19–23, 1988, American Nuclear Society, La Grange Park, IL, 1994, pp. 410–422.
[10] Clayton, J. C., "Internal Hydriding in Irradiated Defected Zircaloy Fuel Rods," *Zirconium in the Nuclear Industry—Eighth International Symposium, ASTM STP 1023*, L. F. P. Van Swam and C. M. Eucken, Eds., ASTM International, West Conshohocken, PA, 1989, pp. 266–288.
[11] Lysell, G. and Grigoriev, V., "Characteristics of Axial Splits in Failed BWR Fuel Rods," *Ninth International Symposium on Environmental Degradation of Materials in Nuclear Power Systems—Water Reactors*, Newport Beach, CA, August 1–5, 1999, The Minerals, Metals and Materials Society, Warrendale, PA, 1999, pp. 1169–1175.
[12] Efsing, P. and Pettersson, K., "Delayed Hydride Cracking in Irradiated Zircaloy Cladding," *Zirconium in the Nuclear Industry—12th International Symposium, ASTM STP 1354*, Toronto, Canada, June 15–18, 1998, G. P. Sabol and G. D. Moan, Eds., ASTM International, West Conshohocken, PA, 2000, pp. 340–355.
[13] Edsinger, K., Davies, J. H., and Adamson, R. B., "Degraded Fuel Cladding Fractography and Fracture Behavior," *Zirconium in the Nuclear Industry—12th International Symposium, ASTM STP 1354*, Toronto, Canada, June 15–18, 1998, G. P. Sabol and G. D. Moan, Eds., ASTM International, West Conshohocken, PA, 2000, pp. 316–339.
[14] Edsinger, K., "A Review of Fuel Degradation in BWRs," *Int. Topical Meeting on Light Water Reactor Fuel Performance*, Park City, April 10–13, 2000, American Nuclear Society, La Grange Park, IL, 2000, pp. 162–179.
[15] Shimada, S., Etoh, E., Hayashi, H., and Tukuta, Y., "A Metallographic and Fractographic Study of Outside-In Cracking Caused by Power Ramp Tests," *J. Nucl. Mater.*, Vol. 327, 2004, pp. 97–113.
[16] Sakamoto, K., Nakatsuka, M., and Higuchi, T., "Simulation of Cracking During Outside-In Type Failure of High Burn-Up Fuel Cladding Tubes," *Water Reactor Fuel Performance Meeting*, Seoul, Korea, October 19–23, 2008, Korean Nuclear Society, Seoul, Korea, 2008, Paper 8009.
[17] Ogata, K., Baba, T., Kamimura, K., Etoh, Y., and Ito, K., "Separate Effects of Factors Affecting Outside-In Cracking of High Burnup Fuel Cladding," *Water Reactor Fuel Performance Meeting*, Seoul, Korea, October 19–23, 2008, Korean Nuclear Society, Seoul, Korea, 2008, Paper 8130.
[18] Unnikrishnan, K., Mishra, P., Jathar, V. P., Kumar, S., Sahoo, K. C., and Anantharaman, S., "Observation of Delayed Hydride Cracking in PHWR Fuel Assembly," *Tenth CNS International Conference on CANDU Fuel*, Toronto, Canada, October 5–8, 2008, Canadian Nuclear Society, Toronto, ON, Canada, 2008.
[19] Coleman, C. E. and Inozemtsev, V. V., "Measurement of Rates of Delayed Hydride Cracking (DHC)

in Zr–2.5Nb alloys—An IAEA Coordinated Research Project," *J. ASTM Int.*, Vol. 5, 2008, paper ID JAI101091.

[20] Efsing, P. and Pettersson, K., "The Influence of Temperature and Yield Strength on Delayed Hydride Cracking in Hydrided Zircaloy-2," *Zirconium in the Nuclear Industry—Eleventh International Symposium, ASTM STP 1295*, Garmisch-Partenkirchen, Germany, September 11–14, 1995, E. R. Bradley and G. P. Sabol, Eds., ASTM International, West Conshohocken, PA, 1996, pp. 394–404.

[21] Grigoriev, V. and Jakobsson, R., "Delayed Hydrogen Cracking Velocity and J-Integral Measurements on Irradiated BWR Cladding," *J. ASTM Int.*, Vol. 2, 2005, paper ID JAI12434.

[22] Grigoriev, V., Josefsson, B., Lind, A., and Rosborg, B., "A Pin-Loading Tension Test for Evaluation of Thin-Walled Tubular Materials," *Scr. Metall. Mater.*, Vol. 33, No. 1, 1995, pp. 109–114.

[23] Grigoriev, V., Josefsson, B., and Rosborg, B., "Fracture Toughness of Zircaloy Cladding Tubes," *Zirconium in the Nuclear Industry—Eleventh International Symposium, ASTM STP 1295*, Garmisch-Partenkirchen, Germany, September 11–14, 1995, E. R. Bradley and G. P. Sabol, Eds., ASTM International, West Conshohocken, PA, 1996, pp. 431–447.

[24] Yagnik, S. K., Ramasubramanian, N., Grigoriev, V., Sainte-Catherine, C., Bertsch, J., Adamson, R., Kuo, R.-C., Mahmood, S. T., Fukuda, T., Efsing, P., and Oberländer, B. C., "Round-Robin Testing of Fracture Toughness Characteristics of Thin-Walled Tubing," *J. ASTM Int.*, Vol. 5, 2008, paper ID JAI101140.

[25] Coleman, C., Grigoriev, V., Inozemtsev, V., Markelov, V., Roth, M., Makarevicius, V., Kim, Y. S., Kanwar, L. A., Chakravartty, J. K., Mizrahi, R., and Lalgudi, R., "Delayed Hydride Cracking in Zircaloy Fuel Cladding—An IAEA Coordinated Research Programme," *Nucl. Eng. Technol.: Int. J. Korean Nucl. Soc.*, Vol. 41, 2009, pp. 171–178.

[26] Grigoriev, V. and Jakobsson, R., "DHC Axial Crack Velocity Measurements in Zirconium Alloy Fuel Cladding," *STUDSVIK/N-05/281*, Studsvik Nuclear AB, 2005, ISBN 91-7010-377-1.

[27] Roth, M., Compliance measurements based on Ref 26, INR, June 23, 2009.

[28] Huang, F. H. and Mills, W. J., "Delayed Hydride Cracking Behavior for Zircaloy-2 Tubing," *Metall. Trans. A*, Vol. 22A, 1991, pp. 2049–2060.

[29] Puls, M. P., Simpson, L. A., and Dutton, R., "Hydride-induced crack growth in zirconium alloys," *AECL Report* AECL-7392, Atomic Energy of Canada Limited, Whiteshell Nuclear Research Establishment, Pinawa, Manitoba, Canada, 1982.

[30] Coleman, C. E., "Effect of Texture on Hydride Reorientation and Delayed Hydrogen Cracking in Cold-Worked Zr–2.5Nb," *Zirconium in the Nuclear Industry—Fifth International Conference, ASTM STP 754*, Boston. MA, August 4–7, 1980, D. G. Franklin, Ed., ASTM International, West Conshohocken, PA, 1982, pp. 393–411.

[31] Coleman, C. E., Cheadle, B. A., Cann, C. D., and Theaker, J. R., "Development of Pressure Tubes with Service Life Greater Than 30 Years," Garmisch-Partenkirchen, Germany, September 11–14, 1995, *Zirconium in the Nuclear Industry—Eleventh International Symposium, ASTM STP 1295*, E. R. Bradley and G. P. Sabol, Eds., ASTM International, West Conshohocken, PA, 1996, pp. 884–898.

[32] Kim, S. S. and Kim, Y. S., "K_{IH} in Radial Textured Zr–2.5%Nb Pressure Tube," *J. Nucl. Mater.*, Vol. 279, 2000, pp. 286–292.

[33] Aomi, M., Baba, T., Miyashita, T., Kamimura, K., Yasuda, T., Shinohara, Y., and Takeda, T., "Evaluation of Hydride Reorientation Behavior and Mechanical Properties for High-Burnup Fuel-Cladding Tubes in Interim Dry Storage," *J. ASTM Int.*, Vol. 5, 2008, paper ID JAI101262.

[34] Sagat, S. and Puls, M.P., "Temperature Limit for Delayed Hydride Cracking in Zr–2.5Nb Alloys," *17th Inter. Conf. Structural Mechanics in Reactor Technology*, Prague, Czech Republic, August 17–22 2003, International Association for Structural Mechanics in Reactor Technology, Berlin, Germany, 2003, Paper G06-4.

[35] Resta Levi, M. and Puls, M. P., "DHC Behaviour of Irradiated Zr–2.5Nb Pressure Tubes up to 365°C," *18th Inter. Conf. on Structural Mechanics in Reactor Technology*, Beijing, China, August 7–12 2005, International Association for Structural Mechanics in Reactor Technology, Berlin, Germany 2005, Paper G10-3.

[36] Mahmood, S. T., Farkas, D. M., Adamson, R. B., and Etoh, Y., "Post-Irradiation Characterization of Ultra-High-Fluence Zircaloy-2 Plate," *Zirconium in the Nuclear Industry: 12th International Symposium, ASTM STP 1354*, Toronto, Canada, June 15–18, 1998, G. P. Sabol and G. D. Moan, Eds.,

ASTM International, West Conshohocken, PA, 2000, pp. 139–169.

[37] Ambler, J. F. R., "Effect of Direction of Approach to Temperature on the Delayed Hydrogen Cracking Behavior of Cold-Worked Zr–2.5Nb," *Zirconium in the Nuclear Industry: Sixth International Symposium, ASTM STP 824*, Vancouver, Canada, June 28–July 1, 1982, D. G. Franklin and R. B. Adamson, Eds., ASTM International, West Conshohocken, PA, 1984, pp. 653–674.

[38] Sagat, S., Chow, C. K., Puls, M. P., and Coleman, C. E., "Delayed Hydride Cracking in Zirconium Alloys in a Temperature Gradient," *J. Nucl. Mater.*, Vol. 279, 2000, pp. 107–117.

[39] Sakamoto, K., Nakatsuka, M., Higuchi, T., and Ito, K., "Role of Radial Temperature Gradient in Outside-In Type Failure of High Burn-Up Fuel Cladding Tubes During Power Ramp Tests," *Proc. Top Fuel 2009*, Paris, France, September 6–10, 2009, French Nuclear Energy Society, Paris, 2009, Paper 2076.